IJAAR PUBLISHING®

West African Journal of Interdisciplinary Research | ISSN: 3027-1878
Volume 2, Issue 2 (April-June, 2024) | www.ijaar.org

Investigation of the properties of oxidized PVC/MWCNT composites with grafted nanographite, focusing on characterization, thermal behavior, and electrical conductivity

[1]Umar Lawan Musa, [2]Hassan Haruna, [3]Dauda Yusuf Tofa, [4]Shafiu Nafiu

[1,2,3,4]Department of science laboratory technology, school of technology, Kano State Polytechnic

Abstract

This research aimed to investigate the influence of nanographite on the thermal and electrical properties of composites made from aminated PVC and oxidized multi-walled carbon nanotubes (MWCNT). DSC analysis showed that the glass transition temperature (Tg) of the aminated PVC was affected by the content of MWCNT in the composites. Higher MWCNT content increased Tg, while lower content decreased it. The addition of nanographite did not significantly alter the initial decomposition temperature, indicating that thermal stability remained unchanged. However, the presence of nanographite increased the residual material at 500°C. Conductivity tests on a specific composite showed that the addition of nanographite improved electrical conductivity, enhancing the material's electrical properties. The conductivity increased with temperature and decreased activation energy with higher frequencies, suggesting easier electron excitation and increased conductivity.

Keywords: PVC (Polyvinyl chloride), MWCNT (Multi-walled carbon nanotubes), Nanographite, Composite materials, Oxidized PVC, Grafted nanographite, Characterization, Thermal behavior, Electrical conductivity

Musa, L. U., Haruna, H., Tofa, Y. D. & Nafiu, S. (2024). Investigation of the properties of oxidized PVC/MWCNT composites with grafted nanographite, focusing on characterization, thermal behavior, and electrical conductivity. *West African Journal of Interdisciplinary Research*. *2*(2), 14-29.

Introduction

Extensive research has been undertaken on metal nanoparticles and nanocomposites, primarily driven by their exceptional properties in the areas of electricity, heat, mechanics, electronics, and optics [1-6]. Promising substrates for polymer composites have emerged, including carbon nanotubes (CNTs) [7, 8], nanographene [9-12], and graphite oxide [13], due to their excellent modulus and conductivity in both electrical and thermal aspects. Carbon nanotubes (CNTs) have particularly captured considerable attention due to their extraordinary physical properties and immense potential in a wide range of nanotechnology applications [14, 15].

The significant obstacle hindering the utilization of carbon nanotubes as drug delivery agents in biological systems is their restricted solubility in organic solvents. This limitation has prompted an increased enthusiasm in altering the surface properties of carbon nanotubes [16-22]. The reason behind this is that surface alteration can enhance their ability to dissolve and interact effectively with different substances, making it easier to separate them using widely available solvents. To enhance their solubility and expand their utility across various applications, numerous approaches for modification have been established, including physical, chemical, and compound methods [23-25]. PVC has gained popularity as a polymer matrix because of its adaptability, cost-effectiveness, chemical durability, and ability to combat bacteria. Moreover, PVC can be conveniently sterilized, making it appropriate for diverse uses. To boost the thermal and mechanical characteristics of PVC, diverse additives are combined with the polymer matrix.

PMMA, also called Polymethyl methacrylate, is a highly adaptable and extensively utilized synthetic resin with notable traits such as outstanding optical transparency, durability, and resistance to weather conditions and chemicals. Expanded graphite, on the other hand, refers to a porous variant of graphite achieved through the mechanical or chemical separation of layers in graphite. When combined, PMMA and expanded graphite showcase exceptional electrical characteristics [48]. Multi-walled carbon nanotubes (MCNT) and reduced graphene oxide (rGO) are two materials showing much promise in improving the electrical characteristics of composites in conjunction with graphite. MCNTs are tubular carbon structures made up of multiple layers of graphene, while rGO is a type of graphene containing functional groups with oxygen that have been eliminated through reduction. Both MCNT and rGO possess distinct electrical, mechanical, and thermal properties that can be utilized to enhance the overall performance of graphite-based composites [49]. The study analyzed how PVC films with different concentrations of multi-walled carbon nanotubes (MWCNTs) absorbed light [42]. The results revealed that higher MWCNT concentrations led to higher light absorption. The efficacy of oleic acid and methyl oleate as dispersants for achieving a homogeneous distribution of MWCNTs in PVC was also investigated and found to be effective [43]. Recent literature has explored the influence of MWCNTs on the properties and structure of PVC composites [44]. Additionally, some studies have incorporated nanographite into polymer composites to enhance their performance, such as reinforcing natural coconut fibers to improve their mechanical properties.

This research aimed to produce composite materials by combining oxidized multi-walled carbon nanotubes (MWCNTs) with a blend of polyvinyl chloride (PVC) and amino compounds (amino PVC). Subsequently, different quantities of nanographite were applied as a coating on the composites. The primary goal of this study was to create composites through a straightforward chemical reaction between the amine groups in PVC and the acid groups in

MWCNTs. Furthermore, the intention was to improve the thermal and electrical characteristics of the composites by incorporating nanographite through grafting.

Experimental

The study utilized oxidized multi-walled carbon nanotubes (MWCNTs) with a carboxyl group concentration of 2.5% obtained from Nanography Co. Ltd. The source of polyvinyl chloride (PVC) was Petkim Nigeria, while synthetic graphite powder with a particle size smaller than 20 μm was also acquired. The molecular weight of cobalt (Co) was estimated to be Mn = 63,000 g mol-1. Various chemicals, including 3-(dimethylamino)1-propylamine, were obtained from Sigma-Aldrich.

Preparation of a PVC compound with the inclusion of an animation process

Initially, amino-based PVC composites with 2% MWCNT were created through a process that involved dissolving 0.49 g of amino PVC in a 10 ml solution of tetrahydrofuran (THF). A 0.01 g amount of oxidized multi-walled carbon nanotubes (MWCNTs) was then added to the aminated PVC solution followed by sonication for an hour. The resulting material was then concentrated in ethanol and then filtered for further use. By employing this approach, we were able to generate PVC/oxidized MWCNT composites comprising varying proportions of oxidized MWCNTs, namely 5%, 8%, and 11%, respectively. After their preparation, all of the composites were dried initially at room temperature. Subsequently, they were further subjected to drying in a freezer at 45°C.

Process of preparing a compound of PVC that has been modified with an amine

To attain the intended result, follow these procedures: Initially, mix 5 grams of PVC, 40 milliliters of 3-(dimethylamino)-1-propylamine, and 9 milliliters of purified water. Utilize a 100 milliliter measuring flask for this blend. Then, expose the mixture to sonication for a period of 5 minutes while allowing argon gas to flow through it. Following this, transfer the beaker containing the solution into an oil bath and agitate it at a temperature of 80 degrees Celsius for an hour. After that, filter the solution using suitable equipment. The amino PVC should be washed with distilled water and ethanol subsequently, and then placed to dry at ambient temperature for a full day. Finally, execute another drying process by immersing it in an environment with a temperature of 45 degrees Celsius for 48 hours [50].

Production process of composites consisting of amino oxidized PVC and MWCNTs

To begin, we created composites of amino-based PVC with 2% MWCNTs. This was achieved by dissolving 0.49 grams of amino PVC in 10 milliliters of tetrahydrofuran (THF). Afterwards, we added 0.01 grams of oxidized multi-walled carbon nanotubes (MWCNTs) to the amino PVC solution and subjected it to sonication for 1 hour. Following this step, the resulting extracts were concentrated in ethanol and then filtered [41]. By following this approach, we successfully produced PVC composites with varying concentrations of oxidized MWCNTs, namely 5%, 8%, and 11% respectively. To ensure effective drying of all preparations, they were first dried at room temperature and later subjected to additional drying in a freezer at 45°C for 48 hours.

Synthesis of composites incorporating oxidized polyvinyl chloride (PVC) and multi-walled carbon nanotubes (MWCNT) in a nanographite form

The mentioned procedure was utilized to fabricate PVC composites containing 8% MWCNT. The process involved the following steps:

- A solution of aminated PVC (0.364 g) was formed by dispersing it in 20 mL of ethanol using an ultrasonic generator for a duration of 90 minutes. This step ensured a homogeneous dispersion.

- Next, the approved PVC dispersion solution was supplemented with oxidized multi-walled carbon nanotubes (MWCNTs) (0.032 g) and nanographites (0.004 g).

- The mixture was then subjected to evaporation and drying under vacuum conditions at 45°C for a total duration of 48 hours. This resulted in the formation of PVC/8% MWCNT composites doped with nanographites.

Additionally, this method was employed to produce composites of PVC/4% and PVC/12% incorporating oxidized nanographites. Different concentrations of nanographites, including 1%, 5%, 8%, and 12%, were utilized in these composites.

Instrumentation

The Perkin-Elmer Spectrum One Fourier Transform Infrared (FTIR) spectrometer was used to collect Infrared (IR) spectra. These spectra were obtained by dispersing potassium bromide (KBr) and measuring wavelengths ranging from 650 to 4000 cm-1. This method of measurement is widely used for discerning the molecular composition and functional groups of a specimen. The calorimetric assessments were carried out utilizing a Shimadzu DSC-50 thermal analyzer designed specifically for this purpose, while nitrogen (N2) gas was utilized to remove any impurities. The samples were gradually heated at a steady rate of 20 °C per minute. The resulting data is frequently utilized for investigating the thermal characteristics of various materials, including their melting points, glass transition temperatures, and heat capacities.

In a previous study, the components of the composite material were blended together using an agate mortar and pestle to analyze their strength. After a thorough mixing process, the resulting powder was subjected to four tons of pressure, yielding thick disk samples. The thickness of these disks varied between 0.40 and 0.67 mm. This method allowed for the assessment of the mechanical properties and overall performance of the composite material. The investigation involved analyzing the total area of the disks, which was found to be 1.13 cm^2, and evaluating how the material's dielectric properties varied with changes in frequency and temperature. To measure the material's behavior, the QuadTech 7600 LRC frequency converter was used, covering a frequency range of 0.1 to 5 kHz. The AC conductivity of the composites was examined at a frequency of 1 kHz and at varying temperatures to assess how the material performs in different conditions. To better understand the arrangement and presence of nanoparticles in the material, scanning electron microscope (SEM) images were captured using a JEOL JSM-7001F instrument. These images were obtained from samples of gold powder, allowing for a comprehensive analysis of nanoparticle distribution and potential effects on the material's properties.

Results and discussion

FTIR AND SEM characterization

In Figure 1, the presented FTIR spectrum shows the aminated PVC/11% oxidized MWCNT composite that has been doped with 12% nanographite. The FTIR spectrum of the doped composite is similar to that of the undoped composite, indicating the presence of similar hydrocarbon groups in both composites.

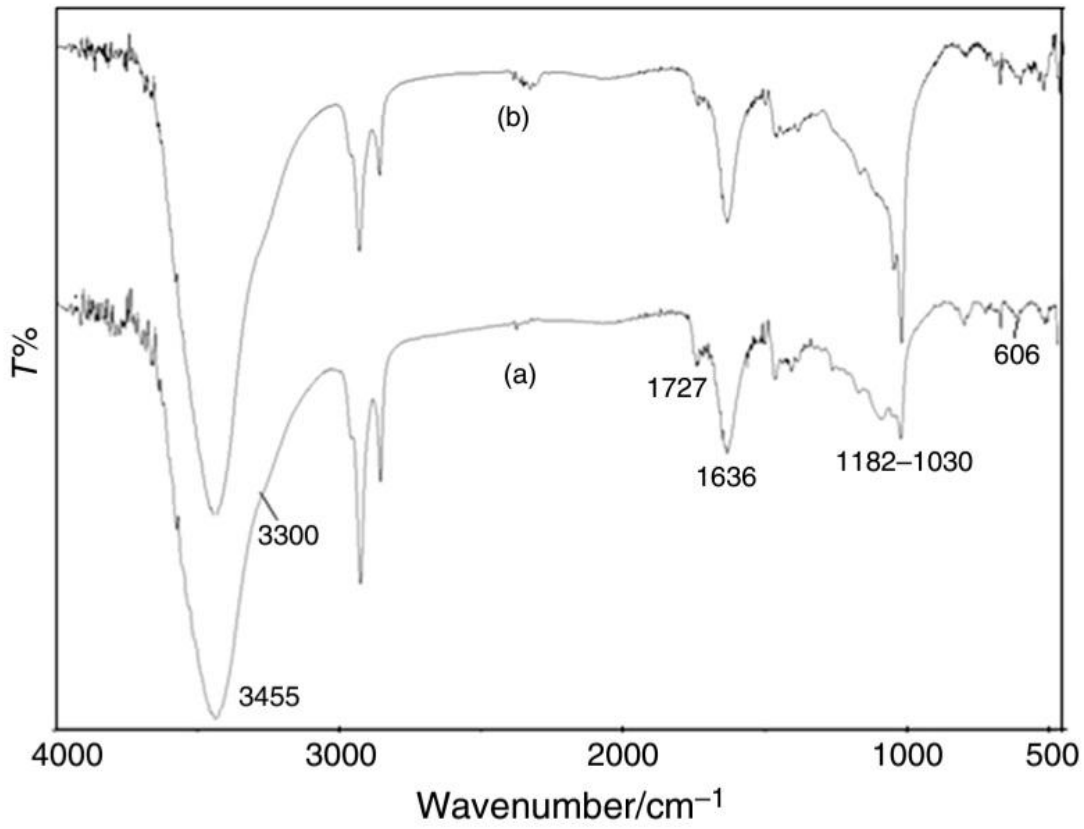


Fig. 1 illustrates the FTIR spectra of two different samples. The first sample is a composite of aminated PVC and 11% oxidized MWCNT, while the second sample is the same composite but doped with 12% nanographite.

Figures 1b and 1c showcase the scanning electron microscope (SEM) images related to the PVC/11% oxidized MWCNT composite. In Figure 1b, the composite is enriched with 3% nanographite, while in Figure 1c, it contains 12% nanographite. These SEM images demonstrate the even distribution of nanofillers throughout the polymer matrix. This suggests that the dispersion process was effective, resulting in a strong interaction between the fillers and the polymer. The fractured regions additionally indicate the existence of empty spaces and fissures, which can be attributed to the fragility of the composite materials. Adding nanographite appears to enhance the ability of the composites to withstand stretching forces and resist fractures. This is evident as the composites with nanographite exhibit less severe fractured regions compared to the pure PVC/11% oxidized MWCNT composite. Generally, the SEM images provide valuable details regarding the shape and internal structure of the composites. This information can be used to guide future refinement and advancement of these materials.

The passage explores the examination of composites that consist of nanographite and oxidized multi-walled carbon nanotube (MWCNT) rods embedded in a polymer matrix. Scanning Electron Microscopy (SEM) is employed to analyze these composites. The SEM images reveal a uniform distribution of the oxidized MWCNT rods and nanographite particles throughout the aminated polyvinyl chloride (PVC) matrix. The oxidized MWCNT rods seem to be not ideally sized as they are being integrated into the polymer matrix. However, the SEM images taken at 50,000 magnifications reveal a consistent scattering of nanographite and oxidized MWCNT particles throughout the aminated PVC matrix. This

indicates that the composite material contains a uniform distribution of nanoparticles, which has the potential to improve its mechanical and electrical characteristics. In Figure 1c, the presence of a significant amount of elevated nanographite content masks or hides the bar structures. This phenomenon happens because the higher concentration of nanographite overpowers the bar structures, resulting in decreased visibility or reduced prominence within the overall structure.

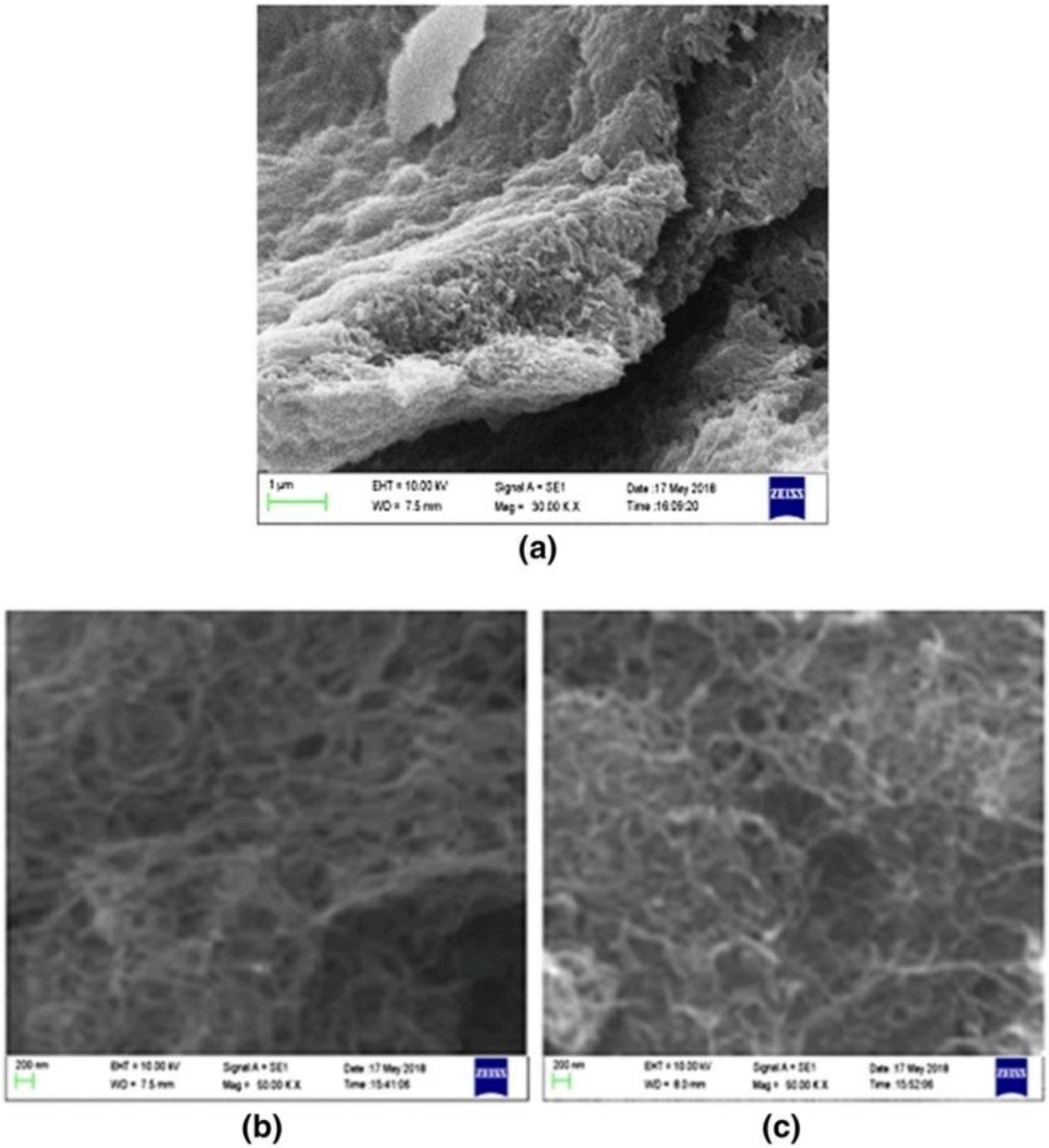


Figure 3 exhibits the DSC plots of composites comprising nanographite-doped PVC with 5% oxidized MWCNTs, showcasing the glass transition temperatures (Tg) observed within the glass transition zone. The values of Tg, identified at the midpoint, have been compiled in Table 1. Prior to introducing graphite, the Tg temperature recorded was 89.5 °C. The Tg temperatures of the graphite-infused composites varied between 85.7 and 87.5 °C. Tables 2 and 3 provide detailed Tg temperatures, extracted from the DSC curves (figures not included), for composites made of aminated PVC/8% oxidized MWCNTs and aminated

PVC/11% oxidized MWCNTs, both doped with nanographite. The Tg temperature indicates the point at which the material undergoes a transition from a glassy, non-crystalline state to a rubbery state. In this study, the Tg temperatures of the composites infused with nanographite were found to range from 86.9 to 89 °C for the composite incorporating 8% oxidized MWCNT, and between 85.7 and 90.7 °C for the composite with 11% oxidized MWCNT. Although the addition of nanographite resulted in a minor alteration of the Tg temperatures in the composites, these adjustments were not significantly significant. This suggests that the addition of nanographite had minimal impact on the Tg temperatures of the composites, indicating that their glass transition properties remained relatively unchanged. It is important to note that the Tg temperature can be influenced by various factors, such as the type and amount of filler used, the level of interaction between the filler and the matrix, and the processing conditions. In this case, although the introduction of nanographite may have caused some modifications in these factors, the overall effect on the Tg temperatures was not significant.

The relationship between Tg temperatures and the nanographite and MWCNT proportions in the composites can be summarized as follows: when the proportion of oxidized MWCNT increases, the Tg temperature of the composites also increases. This phenomenon can be explained by the powerful electrical interaction between the aminated PVC and the oxidized MWCNT, leading to a decrease in the available space within the composite and ultimately raising the Tg temperature. Understanding the behavior of composite materials is essential and can be used to improve their properties for specific purposes. By adding oxidized MWCNT and nanographite to the PVC matrix, the effect on the Tg temperature varies depending on the amount of nanographite present. In the composite with 8% oxidized MWCNT, the glass transition temperature remains mostly unchanged. However, there is a slight decrease in the composite with 5% oxidized MWCNT and a very slight increase in the composite with 11% oxidized MWCNT. These results indicate that the Tg behavior of the composites is significantly influenced by the interaction between the nanomaterials and PVC chains. When a composite with 11% MWCNT incorporates nanographite, it does not cause chain separation. Rather, it occupies the existing area and reduces the amount of free space within the composite. This phenomenon arises from the fact that the aminated PVC and oxidized MWCNT chains have a stronger electrical attraction to each other compared to the nanographite.

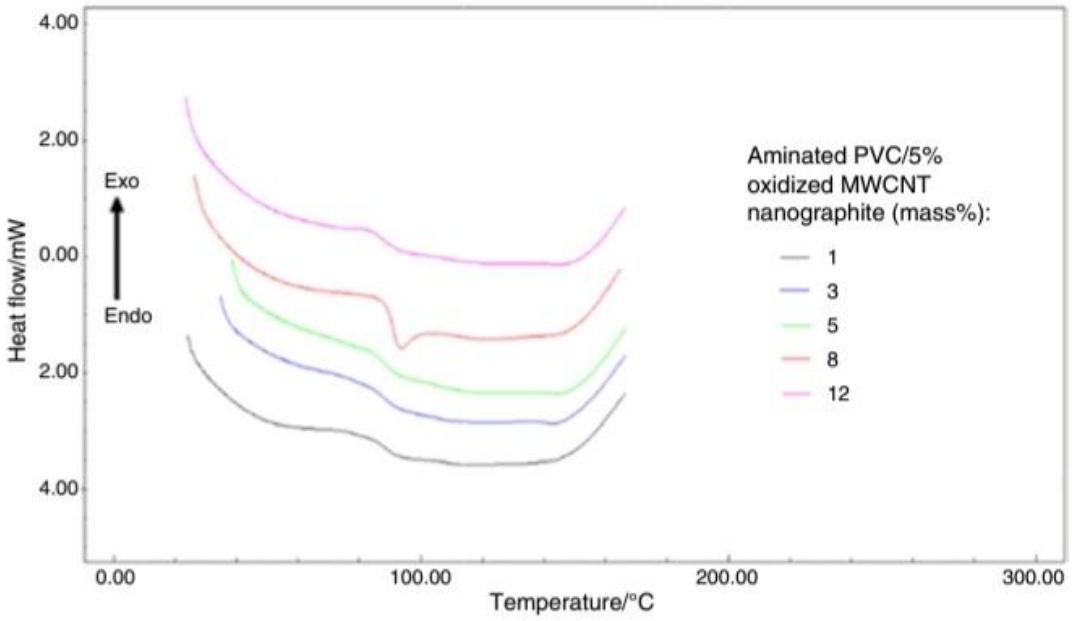


Figure 3 displays the Differential Scanning Calorimetry (DSC) graphs for the composite materials comprising aminated PVC blended with 5% oxidized Multi-Walled Carbon Nanotubes (MWCNTs) and incorporated with nanographite.

Table 1 Thermal investigation of aminated PVC/5% oxidized MWCNT composites doping with nanographite at different percentages

Material	T_g/°C	T_f/°C	Mass loss (mass%) at 300 °C	Residue (mass%) at 500 °C
Amin. PVC/5% MWCNT/nanograph. Comp. nanographite/mass%				
1	86.9	170.0	48.6	27.9
3	86.4	169.0	48.5	29.6
5	85.9	170.0	49.6	31.0
8	87.5	169.6	51.2	32.6
12	85.7	169.8	52.7	34.9

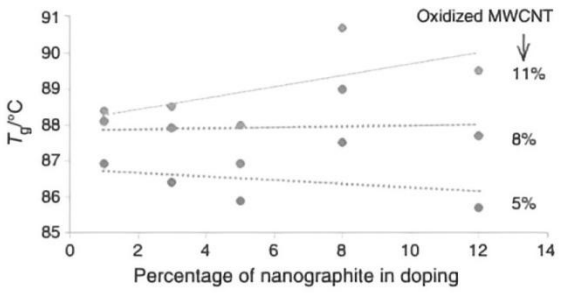


Fig. 4 The effect on T_g temperature of doping with nanographite of aminated PVC/oxidized MWCNT composites

Table 2 Thermal investigation of aminated PVC/8% oxidized MWCNT composites doping with nanographite at different percentages

Material	T_g/°C	T_f/°C	Mass loss (mass%) at 300 °C	Residue (mass%) At 500 °C
Amin.PVC/8% MWCNT/nanograph. Comp. nanographite/mass%				
1	88.1	165	43.0	39.9
3	87.9	168	45.8	37.3
5	86.9	169	44.5	40.6
8	89.0	170	44.2	39.7
12	87.7	168	38.3	47.8

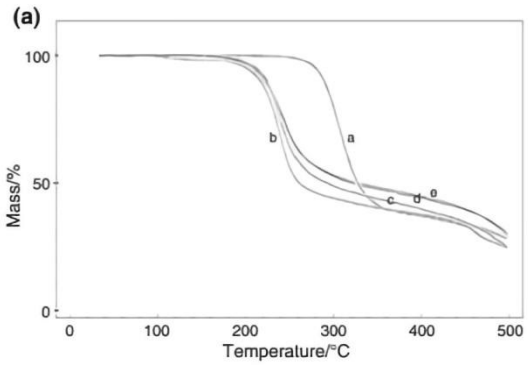


Table 3 Thermal investigation of aminated PVC/11% oxidized MWCNT composites doping with nanographite at different percentages

Material	T_g/°C	T_i/°C	Mass loss (mass%) at 300 °C	Residue (mass%) at 500 °C
Amin.PVC/11% MWCNT/nanograph. Comp. nanographite/mass%				
1	88.4	165	47.1	34.2
3	88.5	165	46.1	32.7
5	88.0	164	45.5	35.9
8	90.7	165	43.0	40.4
12	85.7	166	43.6	39.6

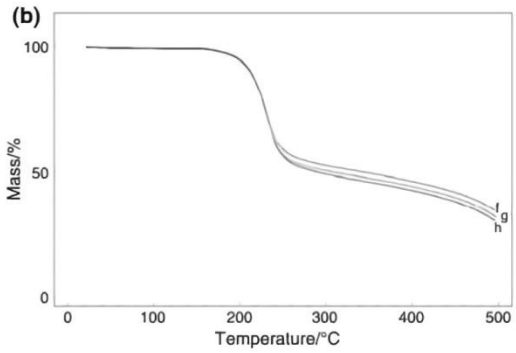


Figure 5: illustrates the thermogravimetric analysis (TGA) curves of several materials. These include (a) PVC, (b) aminated PVC, and composites of aminated PVC/oxidized MWCNTs with varying contents of oxidized MWCNTs (mass%) including (c) 5%, (d) 8%, and (e) 11%. Additionally, TGA curves B represent the aminated PVC/5 mass% oxidized MWCNT composite doped with different percentages of nanographite content (mass%), namely (f) 5%, (g) 8%, and (h) 12%.

Influence of temperature on the electrical conductivity of alternating current (AC)

The main objective of the investigation was to examine how the AC conductivity of a newly developed composite material changes with both frequency and temperature. This composite was made by introducing 8% of aminated PVC/MWCNT with 8% oxidized MWCNT. The AC conductivity of the composite composed of aminated PVC/8% oxidized MWCNT/8% nanographite was measured at different temperatures and frequencies. The results of this experiment are depicted in Figure A, showing a noticeable shift in the relationship between the logarithm of AC conductivity (log σac) and the logarithm of frequency (log ω) at three specific temperatures.

The AC conductivities at 630 Hz (with a linear frequency of 100 Hz) and 15,000 Hz (with a linear frequency of 9550 Hz) are documented as follows: at 20°C, the conductivities are 1.14 × 10−4 S cm−1 and 1.16 × 10−4 S cm−1, respectively; at 50°C, the conductivities are 1.21 × 10−4 S cm−1 and 1.23 × 10−4 S cm−1, respectively; and at 80°C, the conductivities are 1.33 × 10−4−1 and 1.34 × 10−4 S cm−1, respectively. These values indicate that both frequency and temperature have limited influence on the AC conductivity. The equation [54] is used to measure the AC conductivity represented as σac (ω).

The expression σac(ω = dc() → 0) + ac refers to the overall electrical conductivity measurement, where ω represents the angular frequency. Here, σac represents the measured changing electrical conductivity, and σdc signifies the direct contribution to electrical conductivity. At lower frequencies (ω → 0), the σdc(ω) values are determined to be 1.10 × 10−4 S cm−1, 1.19 × 10−4 S cm−1, and 1.29 × 10−4 S cm−1 at temperatures of 20°C, 50°C, and 80°C, respectively. The given data suggests that even though the temperature increased four times, from 20°C to 80°C, the σdc(ω) component of the total conductivity only increased by 17%. However, at 1000 Hz and 20°C, and around 2000 Hz at both 50°C and 80°C, the overall conductivity started to increase with frequency. This observation highlights the frequency-dependent nature of AC conductivity in this specific range. The AC conductivity's variation with frequency can be represented by the equation: ac() = A n (2), where A represents a constant and n denotes the frequency exponent (0 < n < 1). Within the low-frequency range, conductivity escalates as temperature increases, coinciding with the rise in DC conductivity. Conversely, in the high-frequency range, the AC conductivity of the

substance experiences an enhancement as temperature increases. The obtained n values for the implants indicate that the electrical transmission method in these materials is characterized by hopping conductivity, as shown in Figure 6. To calculate the value of n in Equation 2, the slope of the ln(σac) versus ln(ω) graph was examined in the high-frequency range. These determined values were then used to understand the conduction mechanism found in the studied composites [55]. The temperature dependency of the "n" values is illustrated in Figure 7, indicating that the dominant conduction mechanism in these composites is hopping. As the temperature rises, the "n" values decrease and approach zero at high temperatures. Figure 7a represents the relationship between log(σac) and log(ω) for a nanographite-doped composite, while Figure 7b displays the correlation between σac and ω for a composite without nanographite doping at a temperature of 20°C.

This suggests that the materials display an electrical conductivity mechanism based on thermally activated hopping. In Figure 6b, the frequency dependence at 20°C is presented for the composite of aminated PVC/8% oxidized MWCNT, both in its non-doped state and doped with nanographite. The figure demonstrates noticeable distinctions between these two conditions. Moreover, Figure 6b illustrates that the total conductivity at 20°C in the aminated PVC/8% oxidized MWCNT composite without nanographite doping does not include any contribution from DC conductivity. The relationship between conductivity and temperature is described by the Arrhenius equation [57].

$$\sigma = oe^{-Ea/kT}\ \sigma$$

This exhibits direct current (DC) conductivity at lower frequencies and alternating current (AC) conductivity at higher frequencies. σo represents the conductivity at high temperatures, Ea represents the activation energy, and kT is associated with the temperature changes during the measurement. Here, k represents the Boltzmann constant, and T represents the temperature. By performing linear regression on the plot of ln(σ) versus 1000/T, the slope of the Ea values can be determined for different frequencies (as shown in Fig. 8).The minimum energy needed to overcome the obstacle within the composite system, known as the activation energy, is determined by the conductivity and is affected by temperature. Based on the Arrhenius equation, the Ea values obtained from the graph are as follows: 0.0228 eV, 0.0216 eV, 0.0213 eV, and 0.0193 eV at angular frequencies of 630 Hz, 6,900 Hz, 15,000 Hz, and 29,500 Hz, respectively. As evident from these values, the activation energy diminishes as the frequency increases. The higher frequency enables the carrier loads to effortlessly traverse the transmission barriers. Consequently, the activation energy decreases with frequency. Meanwhile, the AC conductivity of the aminated PVC/8% oxidized MWCNT composite was 2.2×10^{-9} S cm^{-1} [58], while the AC conductivity of the 8% doped composite at 20°C increased to 1.15×10^{-4} S cm^{-1}. It has been documented that the conductivity of the composite is magnified by approximately 50,000 times as a result of doping. The AC conductivity values of pure PVC are provided as follows: 1.54×10^{-9} S cm^{-1} at 1/T K 0.0027, 8.85, 0.0029, 0.0031, 0.0033, and 0.0035. At a frequency of 29,500 Hz, the equation $y = -223.94x - 8.30$ ($R^2 = 1.00$) is applicable. At 8,900 Hz, the ln σ values are 8.9, 9, 9.05, and 9.1, with the equation $y = -246.85x - 8.23$ ($R^2 = 0.98$). At 6,900 Hz, the ln σ values are 8.18, 8.22, 8.22, and 8.18 ($R^2 = 0.97$). Moreover, at 630 Hz, the ln σ values are 8.18, 8.22, 8.22, and 8.18 ($R^2 = 0.97$). These values are depicted in Figure 8 [58]. The literature also cites an approximate value of 1.25×10^{-9} S cm^{-1} (at 10 kHz) [59]. In the case of aminated PVC, the AC conductivity is measured at 2.05×10^{-9} S cm^{-1}, while the aminated PVC/8% oxidized MWCNT composite shows an AC conductivity of 2.2×10^{-9} S cm^{-1}. The conductivity enhancement of the oxidized MWCNT was unsuccessful. This lack of effectiveness can be attributed to the increased defects present in the lattice structure of C-C bonds on the surface

of the MWCNTs, which resulted from the acid treatment [60]. Additionally, Thakur and colleagues found that the extended π-conjugation of covalently functionalized MWCNTs composites was disrupted by chemical functionalization, leading to a decrease in their electrical conductivity [61]. In conclusion, aminated PVC composites containing 5%, 8%, and 11% oxidized MWCNTs were doped with nanographite at varying percentages (1%, 3%, 5%, 8%, and 12%).

The thermal stability and glass transition temperatures of PVC/MWCNT composites were not significantly affected by the addition of nanographite. However, the inclusion of nanographite had a considerable impact on the electrical conductivity of the composite. The conductivity increased from 10^{-8} to 10^{-9} S cm-^{1} to 10^{-4} S cm^{-1}, indicating a significant enhancement of electrical conductivity by a factor of 10^{4} to 10^{5}. The doped composite exhibits characteristics of a semiconductor. It is proposed that these composites, studied here, could have promising applications in areas that require the use of semiconductors. The decrease in the exponent values (n) with increasing temperature, and their convergence towards zero at high temperatures, suggest that the materials possess an electrical conductivity mechanism based on thermally activated hopping. Moreover, the activation energy (Ea) for conductivity declined from 0.028 to 0.019 eV, coinciding with an increase in frequency from 630 to 29,500 Hz.

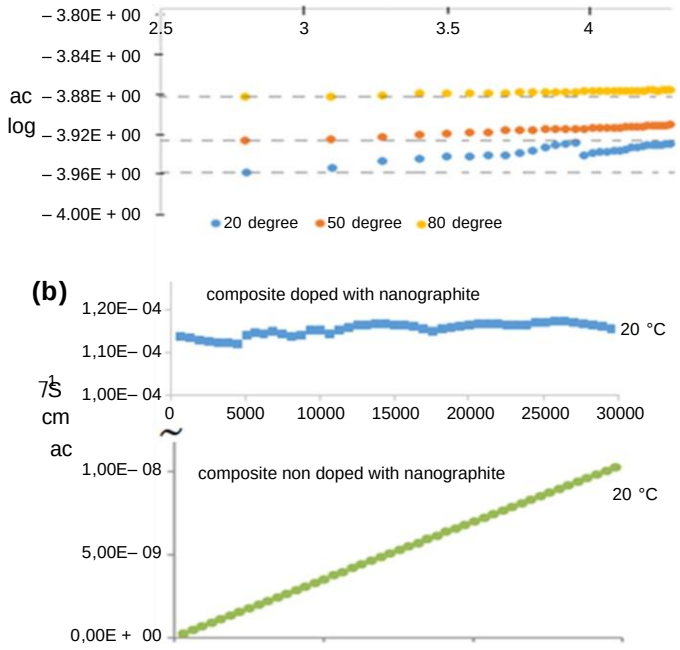


Figure 6 illustrates the changes in AC conductivity of composites consisting of aminated PVC/8% oxidized multi-walled carbon nanotubes (MWCNT)/8% nanographite at various temperatures, measured against frequency. Panel a shows the logarithmic relationship between AC conductivity (σac) and frequency (ω), while panel b depicts the relationship between σac and ω for the composite of aminated PVC/8% oxidized MWCNT at 20°C.

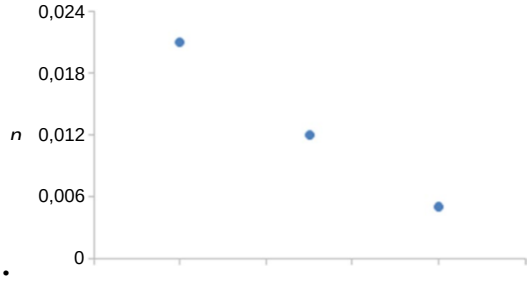


Fig. 7 Temperature dependence of n values

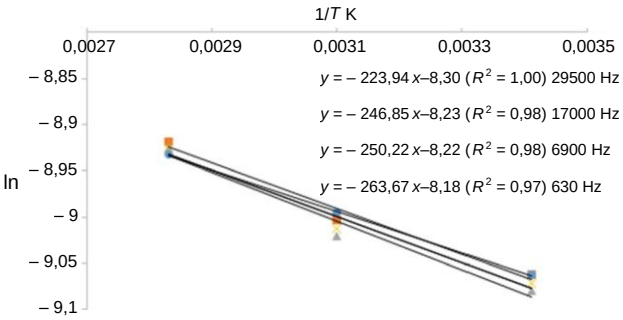


Fig. 8 Ln σ versus 1/T plot at diferent frequencies

CONCLUSION

Different amounts of nanographite (1%, 3%, 5%, 8%, and 12%) were added to composites made of PVC mixed with oxidized PVC at concentrations of 5%, 8%, and 11%. The thermal stability and glass transition temperature of PVC/MWCNT composites containing nanographite were found to be unaffected. However, the electrical properties of the composites show a notable change due to the incorporation of nanographite. The correlation increases from 10-8-10-9 to 10-4 cm-1. This means that the conductivity increases 104-105 times. It has semiconductor-doped properties. It can be said that the compounds investigated in this study have the potential to be used in semiconductor applications in the future. The frequency value, denoted as ‘n’, decreases as the temperature rises, gradually approaching zero at elevated temperatures. This indicates that the material exhibits a conductivity mechanism influenced by temperature changes. Furthermore, the activation energy for conduction, represented as ‘Ea’, decreases from 0.028 eV to 0.019 eV, while the angular frequency increases from 630 Hz to 29500 Hz.

Acknowledgements: The authors would like to extend their appreciation to the Tertiary Education Fund Trust for their support.

References

1. Najafi M, Ansari R, Darvizeh A. Effect of cryogenic aging on nanophased fiber metal laminates and glass/epoxy composites. Polym Compos. 2019;40(6):2523–33.

2. Reddy KR, Karthik K, Prasad SB, Soni SK, Jeong HM, Raghu AV. Enhanced photocatalytic activity of nanostructured titanium dioxide/polyaniline hybrid photocatalysts. Polyhedron. 2016;120:169–74.

3. Reddy KR, Lee K-P, Gopalan AI. Self-assembly directed synthesis of poly (ortho-toluidine)-metal (gold and palladium) composite nanospheres. J Nanosci Nanotechnol. 2007;7(9):3117–25.

4. Reddy KR, Sin BC, Ryu KS, Kim J-C, Chung H, Lee Y. Conducting polymer functionalized multi-walled carbon nanotubes with noble metal nanoparticles: synthesis, morphological characteristics and electrical properties. Synth Met. 2009;159(7–8):595–603.

5. Reddy KR, Lee KP, Gopalan AI. Novel electrically conductive and ferromagnetic composites of poly (aniline-co-aminonaphthalenesulfonic acid) with iron oxide nanoparticles: synthesis and characterization. J Appl Polym Sci. 2007;106(2):1181–91.

6. Reddy KR, Lee K-P, Lee Y, Gopalan AI. Facile synthesis of conducting polymer–metal hybrid nanocomposite by in situ chemical oxidative polymerization with negatively charged metal nanoparticles. Mater Lett. 2008;62(12–13):1815–8.

7. Mamunya Y. Carbon nanotubes as conductive filler in segregated polymer composites-electrical properties. IntechOpen: Carbon nanotubes-polymer nanocomposites; 2011.

8. Reddy KR, Jeong HM, Lee Y, Raghu AV. Synthesis of MWCNTs-core/thiophene polymer-sheath composite nanocables by a cationic surfactant-assisted chemical oxidative polymerization and their structural properties. J Polym Sci Part A Polym Chem. 2010;48(7):1477–84.

9. Son DR, Raghu AV, Reddy KR, Jeong HM. Compatibility of thermally reduced graphene with polyesters. J Macromol Sci Pt B. 2016;55(11):1099–110.

10. Han SJ, Lee H-I, Jeong HM, Kim BK, Raghu AV, Reddy KR. Graphene modified lipophilically by stearic acid and its composite with low density polyethylene. J Macromol Sci Pt B. 2014;53(7):1193–204.

11. Hassan M, Reddy KR, Haque E, Faisal SN, Ghasemi S, Minett AI, et al. Hierarchical assembly of graphene/polyaniline nanostructures to synthesize free-standing supercapacitor electrode. Compos Sci Technol. 2014;98:1–8.

12. Choi SH, Kim DH, Raghu AV, Reddy KR, Lee H-I, Yoon KS, et al. Properties of graphene/waterborne polyurethane nanocomposites cast from colloidal dispersion mixtures. J Macromol Sci Pt B. 2012;51(1):197–207.

13. Lee YR, Kim SC, Lee H-I, Jeong HM, Raghu AV, Reddy KR, et al. Graphite oxides as effective fire retardants of epoxy resin. Macromol Res. 2011;19(1):66–71. 14. Baughman RH, Zakhidov AA, De Heer WA. Carbon nanotubes— the route toward applications. Science. 2002;297(5582):787–92. 15. Kumar NA, Kim SH, Kim JS, Kim JT, Jeong YT. Functionalization of multi-walled carbon nanotubes with cysteamine for the construction of CNT/Gold nanoparticle hybrid nanostructures. Surf Rev Lett. 2009;16(03):487–92.

16. Baskaran D, Mays JW, Bratcher MS. Polymer adsorption in the grafting reactions of hydroxyl terminal polymers with multiwalled carbon nanotubes. Polymer. 2005;46(14):5050–7.

17. Chen Y, Haddon R, Fang S, Rao AM, Eklund P, Lee W, et al. Chemical attachment of organic functional groups to single-walled carbon nanotube material. J Mater Res. 1998;13(9):2423–31.

18. Qin S, Qin D, Ford WT, Resasco DE, Herrera JE. Polymer brushes on single-walled carbon nanotubes by atom transfer radical polymerization of n-butyl methacrylate. J Am Chem Soc. 2004;126(1):170–6.

19. Zou W, Du Z-J, Liu Y-X, Yang X, Li H-Q, Zhang C. Functionalization of MWNTs using polyacryloyl chloride and the properties of CNT—epoxy matrix nanocomposites. Compos Sci Technol. 2008;68(15–16):3259–64.

20. Kong H, Gao C, Yan D. Controlled functionalization of multiwalled carbon nanotubes by in situ atom transfer radical polymerization. J Am Chem Soc. 2004;126(2):412–3.

21. Kumar NA, Ganapathy HS, Kim JS, Jeong YS, Jeong YT. Preparation of poly 2-hydroxyethyl methacrylate functionalized carbon nanotubes as novel biomaterial nanocomposites. Eur Polymer J. 2008;44(3):579–86.

22. Yılmaz S, Coşkun M. Synthesis of an ABC type triblock copolymer on MWCNT Surface: structural, thermal, electrical and SEM characterization. El-Cezerî J Sci Eng. 2017;4:177–89.

23. Mickelson E, Chiang I, Zimmerman J, Boul P, Lozano J, Liu J, et al. Solvation of fluorinated single-wall carbon nanotubes in alcohol solvents. J Phys Chem B. 1999;103(21):4318–22.

24. Saini RK, Chiang IW, Peng H, Smalley R, Billups W, Hauge RH, et al. Covalent sidewall functionalization of single wall carbon nanotubes. J Am Chem Soc. 2003;125(12):3617–21.

25. Foldvari M, Bagonluri M. Carbon nanotubes as functional excipients for nanomedicines: II Drug delivery and biocompatibility issues. Nanomed Nanotechnol Biol Med. 2008;4(3):183–200.

26. Wang Z, Zhang Q, Kuehner D, Xu X, Ivaska A, Niu L. The synthesis of ionic-liquid-functionalized multiwalled carbon nanotubes decorated with highly dispersed Au nanoparticles and their use in oxygen reduction by electrocatalysis. Carbon. 2008;46(13):1687–92.

27. González-Vidal N, de Ilarduya AM, Muñoz-Guerra S, Castell P, Martínez MT. Synthesis and properties of poly (hexamethylene terephthalate)/multiwall carbon nanotubes nanocomposites. Compos Sci Technol. 2010;70(5):789–96.

28. Coşkun M, Yılmaz S. Poli (glisidil metakrilat-ko-stiren): Sentezi, karakterizasyonu, aminlenmiş MWCNT ile reaksiyonu ve termal inceleme. El-Cezeri J Sci Eng 5(2):537–46.

29. Djidjelli H, Martinez-Vega JJ, Farenc J, Benachour D. Effect of wood flour content on the thermal, mechanical and dielectric properties of poly (vinyl chloride). Macromol Mater Eng. 2002;287(9):611–8.

30. Matuana LM, Park CB, Balatinecz JJ. Cell morphology and property relationships of microcellular foamed pvc/wood-fiber composites. Polym Eng Sci. 1998;38(11):1862–72.

31. Peprnicek T, Kalendová A, Pavlová E, Simonik J, Duchet J, Gérard J-F. Poly (vinyl chloride)-paste/clay nanocomposites: investigation of thermal and morphological characteristics. Polym Degrad Stab. 2006;91(12):3322–9.

32. Sun S, Li C, Zhang L, Du H, Burnell-Gray J. Interfacial structures and mechanical properties of PVC composites reinforced by CaCO3 with different particle sizes and surface treatments. Polym Int. 2006;55(2):158–64.

33. Yazdani H, Hatami K, Khosravi E, Harper K, Grady BP. Strainsensitive conductivity of carbon black-filled PVC composites subjected to cyclic loading. Carbon. 2014;79:393–405.

34. Tao Y, Feng W, Ding G, Cheng G. Polyaniline nanorods/PVC composites with antistatic properties. Russ J Phys Chem A. 2015;89(8):1445–8.

35. Conn C, Booth N, Unsworth J. Preparation of a flexible polyaniline-pvc composite. Adv Mater. 1995;7(9):790–2.

36. Ouyang M, Chan CM. Electrical and mechanical properties of pre-localized polypyrrole/poly (vinyl chloride) conductive composites. Polym Eng Sci. 1996;36(21):2676–82.

37. Vadukumpully S, Paul J, Mahanta N, Valiyaveettil S. Flexible conductive graphene/poly (vinyl chloride) composite thin film with high mechanical strength and thermal stability. Carbon. 2011;49(1):198–205.

38. Al-Ramadhan Z, Hashim A, Ali M, Jewad A. Synthesis and study the electrical properties of carbon nanotubes-polyvinylchloride composites. Iraqi J Phys. 2012;10(18):147–50.

39. Saeed AA, Balwa BD. Structural and AC electrical properties of (LDPE-MWCNTs) polymer nanocomposite. J Coll Educ. 2016;5(5):49–62.

40. Abdullah ET, Naje AN. AC electrical and dielectric properties of PVC-MWCNT nanocomposites. Indian J Sci Technol. 2011;4(7):731–5.

41. Mamunya Y, Boudenne A, Lebovka N, Ibos L, Candau Y, Lisunova M. Electrical and thermophysical behaviour of PVC-MWCNT nanocomposites. Compos Sci Technol. 2008;68(9):1981–8.

42. Abdullah ET, Hasan SM, Naje AN. Optical properties of PVCMWCNT nano composites. 2013.

43. Skórczewska K, Chmıelewska D, Pıszczek K, Tomaszewska J. Obtaining PVC/CNT nanocomposites with the use of dispersing agents. Chemic; 2011.

44. Skórczewska K, Tomaszewska J, Piszczek K, editors. Influence of MWCNT on the processing properties and structure of PVC composites. Macromolecular Symposia; 2018: Wiley Online Library.

45. Ahmad MA, Güven G, Sarıkavaklı N. Some features of doping of nano-graphite in natural coir fibre epoxy-composites. Eur J Sci Technol. 2019;15:491–8.

46. Khan U, O'Connor I, Gun'ko YK, Coleman JN. The preparation of hybrid films of carbon nanotubes and nano-graphite/graphene with excellent mechanical and electrical properties. Carbon. 2010;48(10):2825–30.

47. Zhao H, Du A, Ling M, Battaglia V, Liu G. Conductive polymer binder for nano-silicon/graphite composite electrode in lithiumion batteries towards a practical application. Electrochim Acta. 2016;209:159–62.

48. Chen GH, Wu DJ, Weng WG, Yan WL. Dispersion of graphite nanosheets in a polymer matrix and the conducting property of the nanocomposites. Polym Eng Sci. 2001;41(12):2148–54.

49. Guo R, Ren Z, Bi H, Xu M, Cai L. Electrical and thermal conductivity of polylactic acid (PLA)-based biocomposites by incorporation of nano-graphite fabricated with fused deposition modeling. Polymers. 2019;11(3):549.

50. Balakrishnan B, Kumar D, Yoshida Y, Jayakrishnan A. Chemical modification of poly (vinyl chloride) resin using poly